Assessment of a Two-Temperature Kinetic Model for Dissociating and Weakly Ionizing Nitrogen

Chul Park*
NASA Ames Research Center, Moffett Field, California

The validity of a two-temperature chemical/kinetic model is assessed by comparing the calculated results with the existing experimental data for nitrogen in the dissociating and weakly ionizing regime produced behind a normal shock wave. The shock tube radiation program (STRAP) based on the two-temperature model is used in calculating the flow properties behind the shock wave, accounting for the diffuse nature of vibrational relaxation at high temperatures but neglecting the preferential high-vibrational-state removal by dissociation. The nonequilibrium air radiation (NEQAIR) program is used in determining the radiative characteristics of the flow. Comparison is made between the calculated and the existing shock tube data on 1) spectra in the equilibrium region, 2) rotational temperature of the N_2^+ B state, 3) vibrational temperature of the N_2^+ B state, 4) electronic excitation temperature of the N_2 B state, 5) the shape of the time variation of radiation intensities, 6) the times to reach the peak in radiation intensity and equilibrium, and 7) the ratio of nonequilibrium- to equilibrium- radiative heat fluxes. Good agreement is seen between the experimental data and the present calculation except for the vibrational temperature. A possible reason for the discrepancy is given.

Nomenclature

C = reaction rate coefficient, $cm^3/(mole\text{-}s)$
e = radiation power emission, W/cm^3
H_0 = dissociation energy
K = reaction rate coefficient
k = Boltzmann constant = 1.3805×10^{-16} erg/(K)
M = unspecified collision partner
n = preexponential power in rate coefficient expression
p = pressure
T = heavy particle translational and rotational temperature, K
T_v = vibrational, electron-translational, and electronic temperature, K
u = flow velocity, cm/s
x = distance from shock wave, cm
ρ = density, g/cm^3
σ = a constant that characterizes a cross section for electronic excitation of molecules by heavy-particle impact; see Eq. (12)
τ = vibrational relaxation time

Subscripts

a = average between T and T_v; see Eq. (10)
e = equilibrium
s = post-shock condition
∞ = freestream

Introduction

THE concept of the aeroassisted orbital transfer vehicle (AOTV) has been evolving rapidly in recent years.[1-3] Of the two possible basic types of AOTV, namely aeromaneuvering and aerobraking, the aerobraking AOTV is generally expected to encounter a less severe thermal environment for its heat shield than the aeromaneuvering AOTV during its atmospheric flight phase, and therefore to be more easily developed. The aerobrake consists of a blunt body with a large nose-radius, and hence convective heat transfer rates at its stagnation point and elsewhere are likely to be relatively small. Because of the large size, the thickness of the shock layer over the body will also be large, which tends to increase the radiative-heat-transfer rate to the body.

The magnitude of these radiative-heat-transfer rates for the aerobraking AOTV is at present uncertain. The flight altitudes of the AOTV are expected to be high, typically about 80 km. At such high altitudes, air density is low and so the flow in the shock layer over the aerobrake is likely to be in a chemical (and thermal) nonequilibrium state. Controversy has existed since the 1960s on the radiative behavior of gases in such low-density nonequilibrium flows.[4] In laboratory tests using shock tubes, the nonequilibrium phenomenon always led to an increase in radiation emission, but the volume-integrated radiative heat flux remained nearly constant over a range of freestream densities. However, in the flight experiments of Fire and Apollo,[4] the measured radiative heat fluxes were considerably smaller than those deduced from the laboratory experiments. Two different interpretations have been advanced. 1) The collision-limiting theory states that the frequency of molecular collisions at low densities is insufficient to maintain the atoms and molecules in the excited states.[4] 2) The truncation theory states that the cold viscous boundary layer at such low densities extends over most of the shock layer and therefore the shock layer cannot radiate.[4]

The controversy cannot be resolved without further research and experimentation. However, the careful theoretical analysis of the existing data presented here will be useful. It focuses on nitrogen flow only, because the kinetics for nitrogen flow are considerably simpler than for air. The knowledge gained with nitrogen flow will be helpful in understanding the processes in air. During the 1960s, fairly thorough shock-tube tests were carried out by Avco Everett Research Laboratory (in Everett, Mass.) with nitrogen.[5-7] The tested freestream densities corresponded to those usually obtained at 1 to 10 Torr of pressure at room temperature. The tested shock velocities were up to 6.4 km/s. In these thermodynamic environments, the kinetic processes occurring in the flow are 1) vibrational relaxation, 2) substantial dissociation, and 3) weak ionization. The tests produced data on the time variation of vibrational, rotational, and

Presented as Paper 86-1347 at AIAA/ASME 4th Thermophysics and Heat Transfer Conference, Boston, MA, June 2-4, 1986; received July 7, 1986; revision received May 14, 1987.

*Research Scientist. Associate Fellow AIAA.

electronic excitation temperatures; time variation of radiation intensities at several selected wavelength regions; the times to reach the peak in radiation intensity; the times to reach equilibrium; and the ratio of nonequilibrium- to equilibrium- radiative heat fluxes.

The purpose of the present work is to examine how closely the best available theoretical technique reproduces the available experimental data and by confirming that it does, thereby validate the theoretical technique. As noted earlier,[8] there are uncertainties in several physical parameters in the chemical/kinetic model for such environments. In the present work, these unknown parameters are varied until the computed quantities agree with the experimental data. The present work thus serves indirectly to validate those chosen parameters.

The calculation is done using the shock tube radiation program (STRAP) developed previously by the author.[9] Radiative properties are calculated using the nonequilibrium air radiation (NEQAIR) program developed previously also by the author.[10,11]

Method of Calculation

A flowfield through a constant-area duct behind a normal shock wave (as shown at the top of Fig. 1) is analyzed in the present work. The position of the shock wave is assumed to be fixed at $x = 0.05$ cm. The basic governing equations for such a flow in high-temperature, low-density environments have been presented in other studies.[8,9,12] The present analysis is based on the two-temperature model.[9] In the model, the rotational temperature (T) of the molecules is assumed to be equal to the translational temperature of the heavy particles (atoms and molecules). The vibrational temperatures of all molecules in all electronic states are assumed to be the same and to be equal to the translational temperature of the electrons. For the purpose of computing flow properties, the atoms and molecules at the three lowest electronic-excited states are assumed to be excited to the equilibrium values corresponding to the electron temperature. (This last assumption is revoked in calculating radiation; populations of various electronic states are calculated in detail therein.[10,11]) The common vibrational-electron-electronic temperature is denoted by T_v. The calculation is carried out using STRAP.[9] The program accounts for the viscous effects and the shock-slip phenomena caused by the viscous phenomena. In the present work, minor improvements and changes were made to the original STRAP program, as is next described.

Vibrational Model

Appleton[13] has shown that, in the region immediately behind a shock wave in N_2 where the temperature is below approximately 9000 K but dissociation has not yet commenced, that is, in the dissociation incubation region, at least the lowest 10 vibrational states relax with the vibrational relaxation time constant τ given by Millikan and White[14] following the Landau-Teller theory. Based on this finding, Appleton et al.[15] deduced the rate coefficient for the thermal decomposition of N_2 ($N_2 + M \rightarrow N + N + M$) from the rate of disappearance of the eighth vibrational level seen subsequent to the incubation period, for the temperature range of 8000 to 14,000 K, if we assume that the vibrational temperature is the same as the translational temperature during the dissociation process (one-temperature model). Baulch et al.[16] considered the reaction rate coefficient values so deduced to be the most accurate and recommended them for general use.

This simplistic one-temperature description of the coupled-vibrational-dissociation phenomena is subject to several uncertainties, especially at high temperatures (above 14,000 K). The first uncertainty concerns the breakdown of the relaxation time expression of Millikan and White at high temperatures. Reference 8 points out that the expression implies an unrealistically large cross section for vibrational excitation at very high temperatures (temperatures in excess of 40,000 K). Reference 8 then introduces a means of correcting for this deficiency, in which the cross-section value asymptotically approaches a specified value in the limit of an infinitely high temperature. This limiting cross-section value is presently an unknown quantity. In the present work, an effort was made to determine the limiting cross-section value through trial and error by comparing the computed radiation behavior with the behavior observed experimentally in a shock tube. The cross-section value of 10^{-16} cm^2 was found to be most appropriate.

The second problem concerns the depletion of vibrational energy during dissociation. As pointed out by Treanor and Marrone,[17] thermal dissociation of a molecule occurs preferentially from the upper vibrational states. According to the theory, one dissociation event depletes vibrational energy by an amount nearly equal to the dissociation energy of the molecule. Thus, dissociation substantially lowers the average vibrational energy of the molecules as compared to that predicted by the Landau-Teller equation.

The third problem concerns the diffusive nature of vibrational relaxation at high temperatures. It is well known that the populations of the vibrational states during the combined vibrational excitation-dissociation process can only be described accurately by simultaneously solving the equations of conservation of individual vibrational state populations (see, for example, Refs. 18 and 19), that is, the master equations. The system of master equations can be represented approximately by a deffusion equation when the gas temperature is sufficiently large compared with the individual vibrational energy gaps for the vibrational levels to be considered continuously distributed.[20] The diffusive nature originates from the fact that the rate of change of one vibrational state is proportional to the difference between the rate of incoming collisional transitions and outgoing collisional transitions, which is, in turn, proportional approximately to the curvature of the population distribution with respect to the vibrational levels. This diffusive nature additionally reduces the rate of vibrational relaxation at high temperatures[19] as compared to that predicted by the Landau-Teller equation.

The second and the third problems invalidate the underlying assumption used by Appleton et al.[15] and Baulch et al.[16] deducing the rate coefficient from the experiment of Appleton et al. In order to interpret correctly the experiment, one must at the very least know the functional dependence of the rate coefficient on the translational-rotational and vibrational temperatures. Granting that the populations of the lowest few vibrational states can be described by a Boltzmann equation using a unique vibrational temperature, and assuming that the upper levels deviating from the Boltzmann distribution satisfy the quasi-steady-state assumption (that is, the rate of change of the population is negligibly slower compared with the rates of incoming and outgoing collisional transitions), one can show from the general properties of the diffusion equation that the dissociation rate coefficient is a function of the translational-rotational temperature T and vibrational temperature T_v. It is intuitively obvious, however, that a lower T or T_v should result in a lower rate coefficient.

In the dissociation experiment of Appleton et al.,[15] the preferential high-vibrational-state depletion is believed to have occurred substantially. However, the diffusive nature of the relaxation must have been relatively weak because the tested temperatures were only mildly high. Due to the preferential vibrational energy depletion, the vibrational temperature must have been substantially lower than the translational temperature during the course of dissociation, which, in turn, must have reduced the apparent dissociation rate. Because the rate coefficient value was deduced with the rate coefficient assumed to be a function only of the translational-rotational temperature, the preferential vibrational energy depletion phenomenon is believed to be automatically accounted for by accepting the rate coefficient so deduced.

Thus, it is believed that the rate coefficient value of Appleton et al.[15] can be used at temperatures higher than 14,000 K, pro-

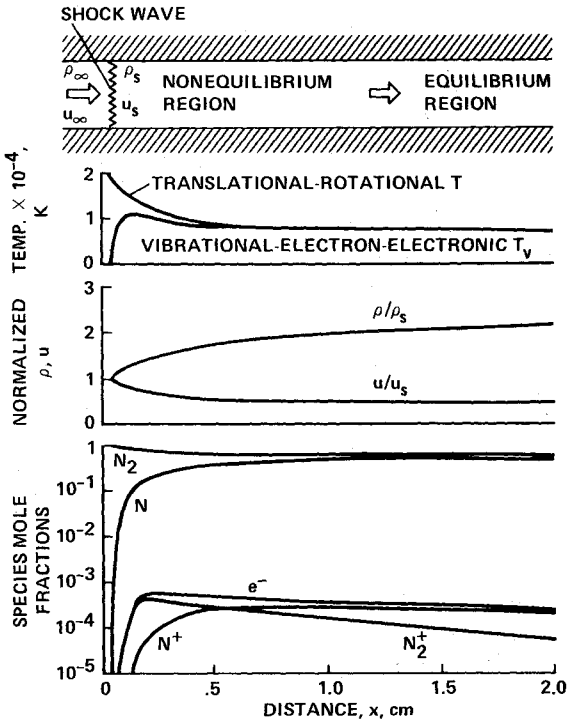

Fig. 1 Schematic of a flow through a constant-area duct (shock tube) and a typical result of calculation; $\rho_\infty = 1.498 \times 10^{-6}$ g/cm^3, $u_\infty = 6.4$ km/s, obtained using the average-temperature reaction-rate model, Eq. (11).

vided the diffusive nature of vibrational relaxation is accounted for. The diffusive nature is accounted for in the present work by using the theoretical results of Lee.[21] For the excitation of vibrational levels of N_2 by collisions of electrons, for which theoretical and experimental excitation cross-section data are available,[21,22] Lee has derived the expression for the vibrational relaxation time. According to the expression, the rate is proportional to an sth power of the difference in temperatures $T_e - T_v$ where T_e is the electron temperature. The exponent s asymptotes to 3.5 at high temperatures (above 10,000 K). The s value of 3.5 evidently results from the diffusive nature of the process. The electron-impact vibrational excitation process is especially diffusive because it is not selective, that is, multilevel transitions are allowed.

The s value for the heavy-particle impacts needed in the present calculation has not been determined because cross-section data for that process are not as reliable as for the electron-impact process. The same s value cannot be used here because the heavy-particle impact process is less diffusive than the electron-impact process because of its selectivity: Heavy-particle impacts favor a vibrational transition to a neighboring level. However, at low temperatures in which the vibrational excitation occurs only to the first vibrational level, s must be unity as the Landau-Teller equation is valid. At the infinitely large temperature, one can infer from Ref. 21 that s must also be 3.5 for the heavy particle-impact excitation process, because the process must be totally diffusive at infinitely high temperature. Therefore, in the present work, the s value is estimated to be unity at 4000 K (the temperature for which most experimental vibrational-excitation-rate data confirm the validity of the Landau-Teller equation), to be 3.5 at infinite temperature, and to obey a linear Arrhenius relationship between these two points. This leads to an approximate expression for s

$$s = 3.5 \times \exp(-5000/T_s) \tag{1}$$

where T_s is the post-shock temperature. The vibrational relaxation time τ thus becomes

$$\tau = \tau_0/[(T_s - T_v)/(T_s - T_{vs})]^{s-1} \tag{2}$$

where τ_0 is the relaxation time appropriate for this Landau-Teller equation, corrected for the high-temperature limit as mentioned previously in the discussion of Ref. 8, and T_{vs} is the post-shock vibrational temperature.

Reaction Model

For nitrogen undergoing dissociation and ionization, the reactions that must be considered are

$$\text{Heavy particle-impact dissociation:} \quad N_2 + M \rightarrow N + N + M \tag{3}$$

where M is an unspecified heavy particle

$$\text{Electron-impact dissociation:} \quad N_2 + e \rightarrow N + N + e \tag{4}$$

$$\text{Associative ionization:} \quad N + N \rightarrow N_2^+ + e \tag{5}$$

$$\text{Charge exchange:} \quad N_2 + N^+ \rightarrow N_2^+ + N \tag{6}$$

$$\text{Electron-impact ionization:} \quad N + e \rightarrow N^+ + e + e \tag{7}$$

Both the forward and reverse rates of the reactions (4) and (7) are determined only by the electron temperature, whereas those of reaction (6) are probably determined only by the heavy-particle translational temperature. For reaction (5), the forward rate is determined by the heavy-particle translational temperature, whereas the reverse rate is determined by the electron temperature. For the dissociation reaction (3), which is most important in terms of the energy involved, the reverse rate is dictated by T. But the expression for the forward rate coefficient is presently indeterminable because it is likely to be affected significantly by both T and T_v. In previous works, the author proposes two different forms of functional dependence of the rate coefficient on the two temperatures.[8,9] Reference 23 points out inadequacies in both forms. In the present work, therefore, three different forms, based on three different kinetic models, are tested.

One-temperature Model

In this model, the vibrational-electron-electronic temperature T_v is assumed to be the same as the heavy-particle translational-rotational temperature T, in calculating both flow properties and reaction rates. The rate coefficient of dissociation then becomes

$$K = CT^n \exp(-H_0/kT) \tag{8}$$

where C is the rate constant, n the preexponential power, and H_0 the dissociation energy.

Vibrational Temperature Model

In this model, vibrational-electron-electronic temperature T_v is assumed to dictate the rate coefficient, so that

$$K = CT_v^n \exp(-H_0/kT_v) \tag{9}$$

This model would be accurate if dissociation was caused solely by the breakage of the bond from vibrational stretching.

Average Temperature Model

In this model, the rate coefficient is assumed to be dictated by the (geometric) average temperature

$$T_a = \sqrt{T \times T_v} \tag{10}$$

Table 1 Rate constants used

Reaction	C, $cm^3\ mole^{-1}\ s^{-1}$	n	H_0/k, K	Reference
$N_2 + N_2 \rightarrow N + N + N_2$	3.70×10^{21}	−1.6	113,200	15, 16
$N_2 + N \rightarrow N + N + N$	1.66×10^{22}	−1.6	113,200	24
$N_2 + e \rightarrow N + N + e$	8.30×10^{24}	−1.6	113,200	Present work
$N + N \rightarrow N_2^+ + e$	1.79×10^{11}	−0.77	67,500	25
$N_2 + N^+ \rightarrow N_2^+ + N$	9.85×10^{12}	−0.18	12,100	See text
$N + e \rightarrow N^+ + e + e$	2.50×10^{10}	−3.82	168,600	2 × Ref. 26

in the form

$$K = CT_a^n \exp(-H_0/kT_a) \tag{11}$$

This model allows dissociation of a molecule by both centrifugal tearing caused by rotational motion and vibrational bond-breaking. The square root of T is a measure of the velocity associated with the rotational motion, whereas the square root of T_v is a measure of the velocity associated with the vibrational motion at the midpoint of its range. The product conceptually represents an average energy level in the phase space where the two velocities form separate momentum coordinates. The rate expression is also fairly close to the form recommended in Ref. 23.

The rate constants C, n, and H_0/k have partly been taken from the existing literature[15,16,24–26] and partly fitted in the present study. They are summarized in Table 1. For the thermal dissociation process (3), the values measured by Appleton et al.[15] and recommended by Baulch et al.[16] and Flagan and Appleton[24] have been used for the reasons given earlier. For the electronic-impact dissociation (4), the best-fit value of C was deduced in the present work by comparing the calculated radiation behavior with the experimental data to be discussed later. For the associative ionization reaction (5), the constants are deduced from the work of Dunn and Lordi.[25] For the charge-exchange reaction (6), the rate constants were deduced from the reverse rate of C, which was deduced from the assumption that the reaction takes place with a cross section of 10^{-16} cm^2. For the electron-impact ionization process (7), the C value in the work of Park[26] was multiplied by a factor of 2 to obtain the best fit to the experimental data. The impact of the present choice of the rate coefficient values are described later in the discussion section.

Heavy Particle-Impact Excitation

In the original NEQAIR program,[11] excitation of electronic states of molecules is assumed to be caused entirely by the collisions of electrons with the molecules. However, in the low end of the velocity regime considered in the present work ($u_\infty = 4.75$ km/s), excitation by heavy-particle impact may be significant. Flagan and Appleton[24] deduced the excitation rate coefficients for the B states of N_2 and N_2^+ from the observed behaviors of radiation of N_2 first positive and N_2^+ first negative bands at relatively low temperatures, that is, at post-shock temperatures below 14,000 K. However, these excitation rate values proved to be too small. According to the present calculation, the rates of increase in the excitation temperatures calculated using these rate coefficients are much slower than those observed in the shock-tube experiments. The best agreement between the calculation and experiment occurs when the much larger excitation rate coefficients next given are used.

For the electronic excitation of any neutral species, the cross section is zero at the threshold and behaves approximately as (e.g., Ref. 27)

$$\text{Cross-section} = \sigma\, \ell n(y)/y \tag{12}$$

where y is the ratio of the translational kinetic energy of the colliding particles to the threshold energy and σ is a constant typically of the order of 10^{-16} cm^2. For a trial, Eq. (12) with a σ value of 10^{-16} cm^2 was adopted for electronic excitation of all transitions in the neutral molecule N_2. For ionic molecules, excitation cross sections are finite at the threshold.[27] As the largest contribution to the rates is usually made at the collision energies equal to or slightly greater than the threshold energies, the cross-section value may be assumed to be a constant at the threshold value. In the present work, the cross section is assumed to be 10^{-17} cm^2, which is a typical value.[27] The heavy particle-impact excitation processes are significant only at low-shock velocities (below 5.5 km/s). At higher velocities, calculations show that excitation of molecular electronic states is caused primarily by electron impact; hence, the uncertainty in the cross-section values for the heavy particle-impact excitation is immaterial.

The difference between the cross-section values deduced by Flagan and Appleton and those chosen in the present work may be attributed to the different treatment of vibrational excitation processes: Unlike the present work, Flagan and Appleton assumed that vibrational excitation reached equilibrium with the heavy-particle translational temperature before electronic excitation of molecules began.

Treatment of Radiation

In the original NEQAIR program,[11] the intensity factors for molecular radiation, that is, the sums of electronic transition moments-squared, are those by Allen.[28] In the present work, they are replaced by the more recent values by Cooper,[29] all in atomic units: 1.25 for N_2^+ first negative band; 3.5 for N_2 second positive band; and 0.5 for N_2 first positive band, respectively. For atomic radiation, the values contained the NEQAIR program are used.

In the original STRAP program,[9] energy loss by radiation was neglected. As described in Ref. 12, energy loss by radiation affects both the total energy and vibrational electron-electronic energy. In the present work, the energy loss term was added in the two conservation equations as prescribed in Ref. 12. The calculation was carried out in an iterative fashion: For the first calculation, radiation was neglected. Radiation power loss was then calculated for the converged solution, and the radiative loss term was then accounted for in the next calculation by assuming nitrogen to be optically thin. The effect of radiative power loss on flow properties was seen to be very small in the present ranges of interest, and hence, only one such iteration was necessary.

In the experiments,[5,7] radiation was observed through a slit of 0.05 cm width. The calculation of radiation was made with allowance for a slit function consisting of a Gaussian profile of 0.05 cm full half-width. Also, radiation was seen to increase approximately linearly with distance from the shock wave after the flow reached equilibrium.[5] This phenomenon is attributable to the growth of boundary layers on the wall of the shock tube, which causes an adiabatic compression of the flow. This effect was accounted for in the present calculation by assuming the density and the two temperatures increased at the rate of 2.5 and 1% per cm, respectively, beyond the values calculated by the STRAP code, starting from the shock wave, for all cases.

Results

The result of a typical calculation, the case of $\rho_\infty = 1.498 \times 10^{-6}$ g/cm^3 (pressure of 1 Torr at room temperature) and $u_\infty = 6.4$ km/s, is shown in Fig. 1. The average-temperature model, Eq. (11), was used for computing reaction rates for this case. As seen in the figure, the vibrational-electron-electronic temperature T_v is significantly lower than the translational-rotational temperature T in the first 1 cm. In this region, T_v is raised through the collisional processes. Density and velocity change by a factor of two. Dissociation of N_2 is significant and the molar fraction of N almost reaches 0.5, but ionization is fairly weak at the calculated conditions.

In Fig. 2, the calculated radiation spectrum is compared with the measured spectrum in the equilibrium region for the case of $\rho_\infty = 1.498 \times 10^{-5}$ g/cm^3 (10 Torr pressure) and $u_\infty = 4.8$ km/s. Both calculation and experiment were made at 200-Å intervals using a monochromator with a wavelength bandwidth of 200 Å starting at 3100 Å. As seen here, the measured data are reproduced by the calculation fairly accurately, that is, within the accuracy of the measurement. This adds support to the method of computing radiation using the NEQAIR program, at least for known thermodynamic conditions.

In Fig. 3, the measured rotational temperature is compared with the translational-rotational temperature calculated in the present work using the three different reaction-rate models, Eqs. (8), (9), and (11). The experimental temperature values are determined from the ratios of the intensities of the radiation from the (0,1) band of the N_2^+ first negative system measured at 4266 and 4243 Å. Unfortunately, the experimental procedure for converting the ratios to rotational temperatures amplifies any experimental error by an order of magnitude. This error-amplification phenomenon causes the relatively large scatter in the experimental data. Because of this large scatter, the experimental data cannot resolve the validity question between the average-temperature model [Eq. (11)] and the vibrational temperature model [Eq. (9)]. However, the figure proves that the scale of relaxation of translational-rotational temperature is approximately reproduced by both models.

In Fig. 4, the measured vibrational temperatures are compared with the calculated vibrational-electron-electronic temperatures. Here, the measured temperatures are those of the N_2^+ B state (the upper electronic state of the N_2^+ first negative system), and the theoretical values are the vibrational temperatures common to all molecules in all electronic states. The experimental data completely disagree with the calculated values. This proves that the present assumption that vibrational temperatures of all molecules in all electronic states are the same is most likely wrong. A more sophisticated model in which vibrational temperatures of the different molecules and different electronic states are separately calculated would be necessary to describe the observed phenomenon. This inadequacy in the present model is not likely to affect other aspects of the problem, however. Most of the vibrational energy is contained in the ground electronic state of the N_2 molecule. The method of treating vibrational energy described in Refs. 9 and 12 and adopted here strictly applies only to the ground electronic state. As long as the ground electronic state is correctly treated, the flow energies and associated reaction rates would be correctly represented. The only quantity the vibrational temperature of the N_2^+B state will affect is the spectral intensity distribution of the N_2^+ first negative system. According to the procedure adopted in the NEQAIR program, the wavelength-integrated intensity of a band system is determined mainly by the electronic excitation temperature of the upper state; the vibrational temperature of the upper electronic state affects only spectral distribution of the integrated intensity. However, the discrepancy seen in Fig. 4 leaves the present vibrational model unverified.

In Fig. 5, the excitation temperature of the N_2 B electronic state, as determined from the integrated intensities of the N_2 first positive system using the NEQAIR program, is compared between the theory and experiment. As mentioned briefly in the beginning of the method of calculation section, the NEQAIR program calculates electronic excitation temperatures from the first principles using the nonequilibrium thermodynamic properties obtained by solving the flow equations. Hence, the results shown in Fig. 5 are free of the assumption made in the flow calculation that the first three electronic excited states are in equilibrium with the ground state at the vibrational-electron-electronic temperature T_v. In Fig. 5, the average-temperature model is seen to be in closest agreement with the experimental

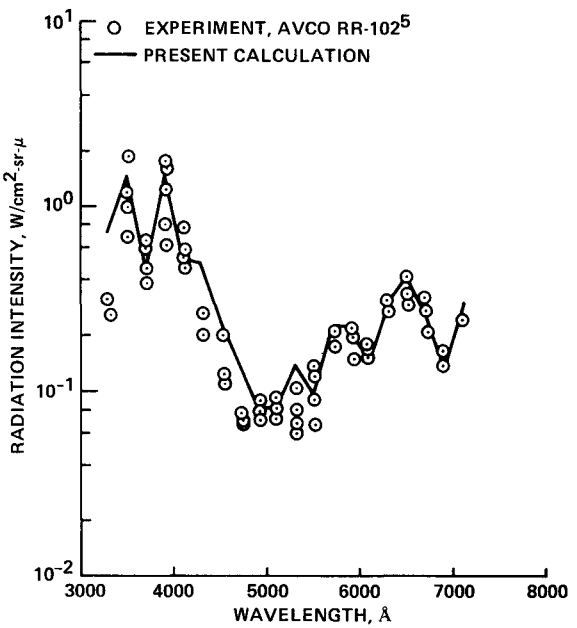

Fig. 2 Comparison between the measured and calculated spectra for an equilibrium region behind a shock wave; $\rho_\infty = 1.498 \times 10^{-5}$ g/cm^3 and $u_\infty = 4.8$ km/s. The wavelength intervals and passband are both 200 Å.

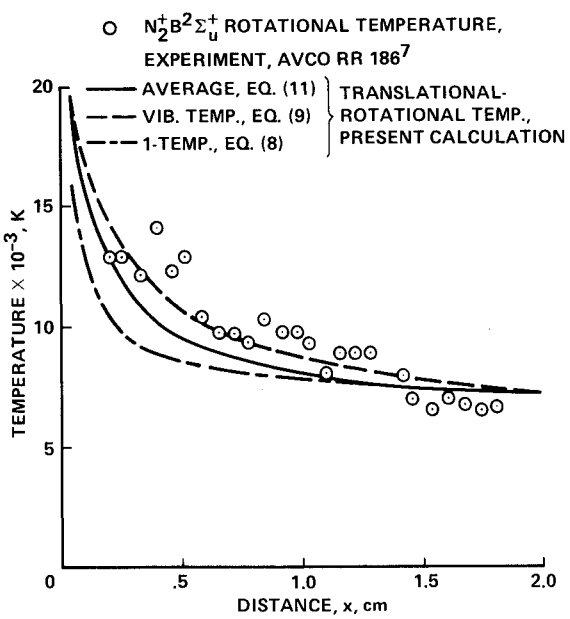

Fig. 3 Comparison between the measured rotational temperature of the N_2^+ B state and the translational-rotational temperature calculated using the three reaction-rate models, Eqs. (8), (9), and (11); $\rho_\infty = 1.498 \times 10^{-6}$ g/cm^3 and $u_\infty = 6.4$ km/s.

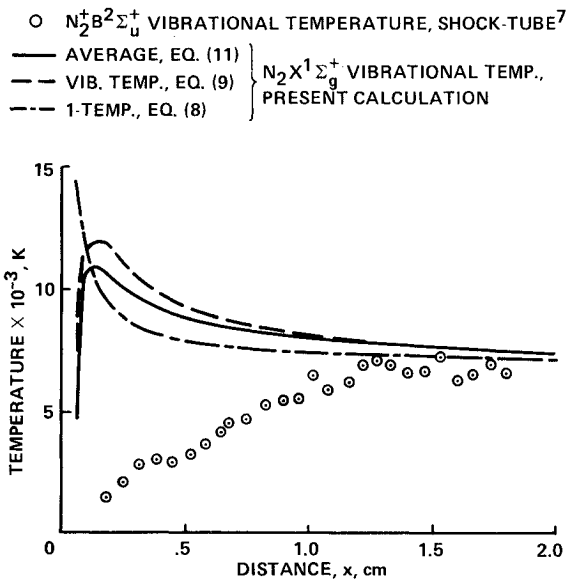

Fig. 4 Comparison between the measured vibrational temperature of the N_2^+ B state and the vibrational temperatures (of the ground electronic state of the N_2) calculated using the three reaction-rate models; $\rho_\infty = 1.498 \times 10^{-6}$ g/cm^3 and $u_\infty = 6.4$ km/s.

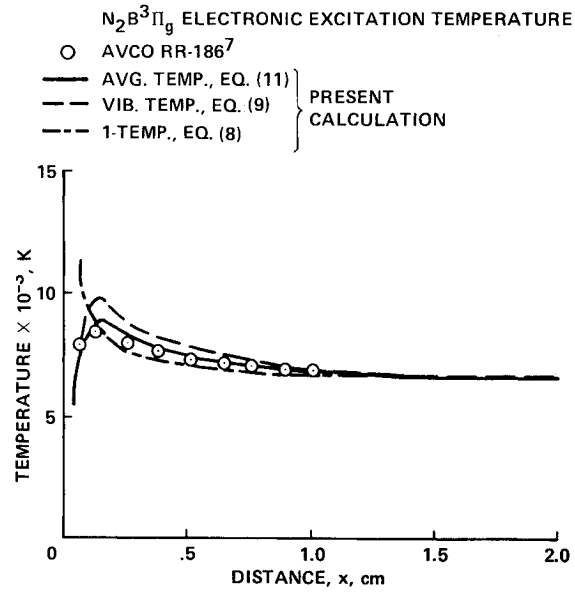

Fig. 5 Comparison between the measured electronic excitation temperature of the N_2 B state and the excitation temperature calculated using the three different reaction-rate models; $\rho_\infty = 1.498 \times 10^{-6}$ g/cm^3 and $u_\infty = 6.4$ km/s.

data. The theoretical values are not affected significantly by the uncertainty in the electronic excitation cross sections for heavy-particle impacts [see Eq. (12)] at $u_\infty = 6.4$ km/s, as the electron-impact excitation process is dominant over the heavy particle-impact process here.

In Fig. 6, the distance- or time-history of the variation of radiation intensity in the wavelength range of 5500 to 10,000 Å, which is produced mainly by the N_2 first positive system, is compared between the theory and experiment. The calculation is made using the three reaction-rate models. As the figure shows, the computed time-history of the radiation intensity agrees most closely with the experimental data when the dissociation rate is calculated using the average-temperature model given by Eq. (11): Only the theoretical calculation made using this model correctly reproduces the ratio between the peak and the asymptotic plateau intensity value and the profile of variation.

In Fig. 7, the calculated and measured histories of radiation intensities are compared at 4266 and 4243 Å, which represent different rotational lines within the (0,1) band of the N_2^+ first negative system, with a wavelength pass band of 5 Å. Here, the average-temperature model, Eq. (11), is used in the calculation. As the figure shows, the calculated temporal variation agrees closely with the experimental results: Not only the general shapes, but the peak intensity points are correctly reproduced by the calculation.

In Fig. 8, the two characteristic radiation relaxation times, that is, the times to reach the peak in radiation intensity and the times to reach the intensity 1.1 time the equilibrium values, are compared between the theory and experiment over a wide range of freestream velocities. The relaxation times are those of the radiation in the wavelength range from 5500 to 10,000 Å. The theoretical values at $u_\infty = 4.75$, 5.54, and 6.4 km/s are calculated using the same freestream density values as in the experiment,[7] that is, those corresponding to 10, 3, and 1 Torr at room temperature, respectively. All three reaction models predict the characteristic times approximately correctly at the low-shock velocity $u = 4.75$ km/s. But at higher velocities, the one-temperature model underestimates the relaxation times significantly. The vibrational temperature model, Eq. (9), and the average-temperature model, Eq. (11), agree equally well with the experimental data. At $u_\infty = 4.75$ km/s, the calculated peak point value was found to be determined mostly by the choice of the cross-section values for excitation of molecular electronic states by the impacts of heavy particles [see Eq. (12)]. The good agreement between the calculated and the experimental results at this velocity validates the cross-section values chosen. To provide a basis for future experimental comparison, the calculation was made also at 8 km ($\rho_\infty = 4.494 \times 10^{-7}$ g/cm^3) and 10 km/s ($\rho_\infty = 1.498 \times 10^{-7}$ g/cm^3).

In Fig. 9, the ratios of nonequilibrium-to-equilibrium radiative heat fluxes in the wavelength range from 5500 to 10,000 Å, calculated under the assumption that the gas is optically thin, are compared between the theory and experiment. The radiative heat flux at any given point can be represented approximately in the present environment using the infinite-slab approximation by half the radiation emission power integrated over the distance from the shock wave to that point. The nonequilibrium-radiative heat flux is defined[4,6,7] as this flux integrated to the point where the intensity reaches 1.1 times the equilibrium value. If we denote emission power by e and the equilibration point by subscript e, the nonequilibrium-to-equilibrium radiative heat-flux ratio becomes

$$\text{nonequilibrium-to-equilibrium radiative heat-flux ratio} = \int_0^{x_e} e \frac{dx}{e_e x_e}$$

Figure 9 shows a relatively large scatter in the experimental data. As the nonequilibrium flux values are relatively easy to measure accurately, the scatter is believed to be due to the errors in the determination of the equilibrium flux values. The equilibrium flux values are determined from the radiation intensity levels at their plateaus in their time-history records (oscillograms). The plateau values are affected at least by two known shock-tube imperfection phenomena: The first is the boundary-layer growth on the wall that changes the test gas properties; the second is the mixing with the driver gas that cools the test gas and sometimes introduces luminous impurity species. As the figure shows, all three models are equally valid at the low-shock velocity, but the average temperature is discernibly better at the high velocity. The agreement is to within

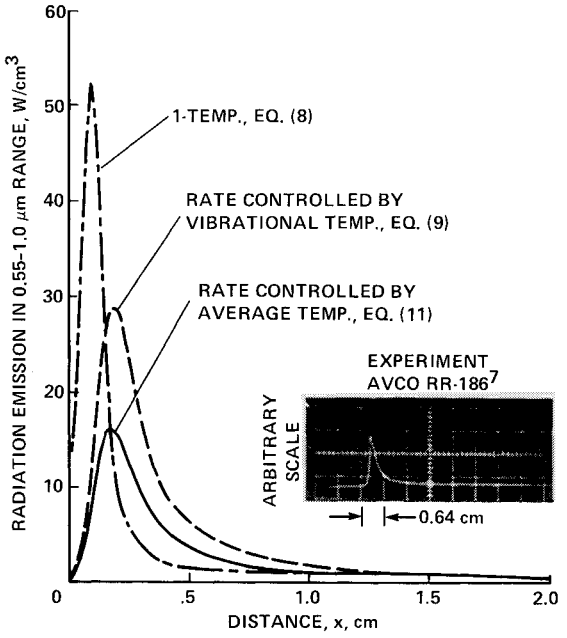

Fig. 6 Distance- or time-history of intensity of radiation from the 5500 to 10,000 Å wavelength range calculated using the three reaction-rate models, compared with the experimental data; $\rho_\infty = 1.498 \times 10^{-6}$ g/cm³ and $u_\infty = 6.4$ km/s.

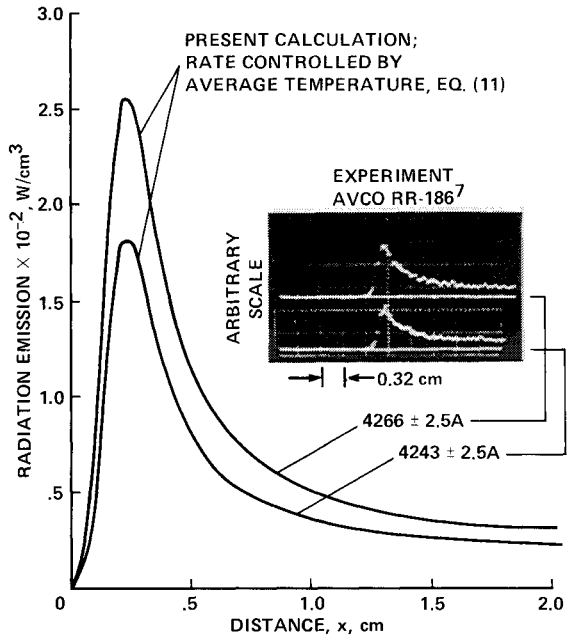

Fig. 7 Distance or time history of intensity of radiation from the 4266 and 4243 Å with a passband of 5 Å calculated using the average-temperature reaction-rate model, Eq. (11), compared with the experimental data; $\rho_\infty = 1.498 \times 10^{-6}$ g/cm³ and $u_\infty = 6.4$ km/s.

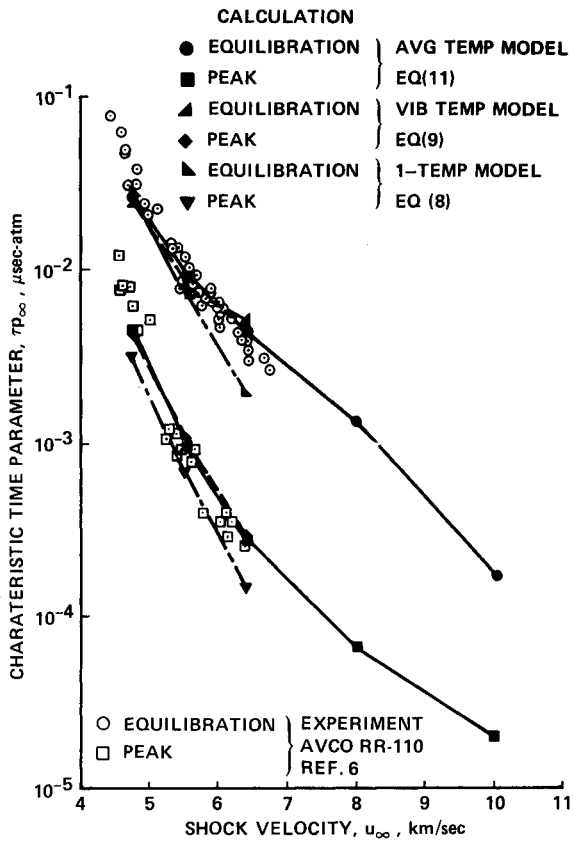

Fig. 8 Comparison between the measured and calculated characteristic relaxation times (the time to the peak radiation point and the time to the point where the intensity is 1.1 times the equilibrium value) of the radiation in the wavelength range from 5500 to 10,000 Å calculated using the three reaction-rate models, compared with the experimental data.

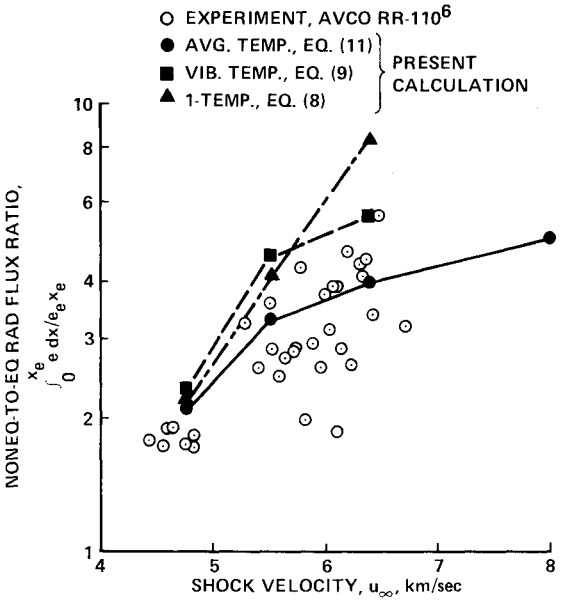

Fig. 9 Comparison between the measured ratios of nonequilibrium-to-equilibrium radiative heat fluxes for the wavelength range of 5500 to 10,000 Å and those calculated using the three reaction-rate models.

the experimental scatter for the average-temperature model.

In Fig. 10, radiative heat fluxes and characteristic relaxation distances calculated by the average-temperature model are shown for various freestream densities and velocities. The calculation was made in order to provide directions for future studies, both theoretical and experimental, of the flow regimes beyond those considered in the foregoing comparison. The radiative heat fluxes in the upper part of the figure are determined through the same integration procedures used in producing the data shown in Fig. 9. However, unlike the Fig. 9 data, the radiation intensity values include those from all possible radiation mechanisms considered in the NEQAIR program. The radiative heat fluxes are almost constant at high

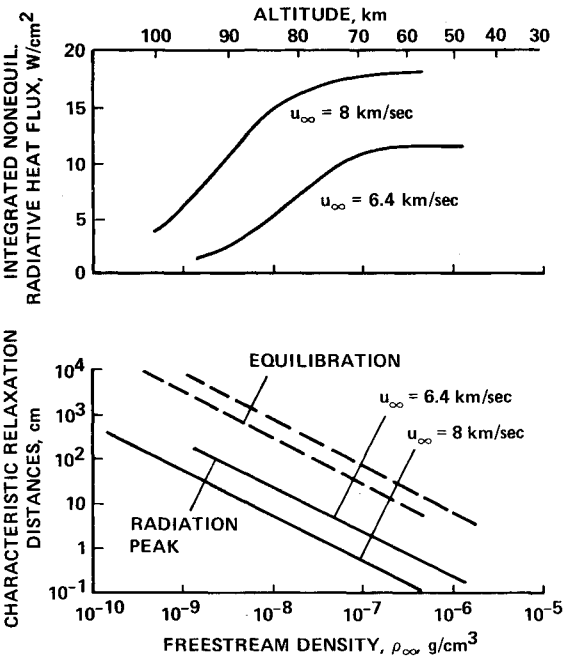

Fig. 10 Nonequilibrium-radiative heat fluxes and characteristic relaxation distances calculated with the average-temperature reaction model, over varying freestream densities.

densities, but decrease as freestream density decreases below certain points. The flat region occurs according to the binary scaling law.[4] The decrease at low densities is caused by the collision-limiting phenomenon.[4] The plot of the characteristic relaxation distances at the lower part should be useful in estimating the shock stand-off distance at which the nonequilibrium-radiative heat flux is expected to become smaller than the full integrated value shown in the upper part. When the stand-off distance is smaller than the equilibration distance, the actual radiative heat flux reaching the wall will be reduced because the relaxation phenomenon will be truncated.

Discussion

From the foregoing comparison between the theoretical and experimental results, it is clear that the average-temperature model expressed by Eq. (11) yields the closest agreement with the existing experimental data. The method closely reproduces the temporal variation of the electronic excitation temperature of the N_2 B state (Fig. 5), radiation intensities at three selected wavelength ranges (Figs. 6 and 7), and the characteristic relaxation times (Fig. 8). It also reproduces the measured rotational temperatures (Fig. 3) and the ratios of nonequilibrium- to equilibrium-radiative heat fluxes (Fig. 9) to within the accuracy of the experimental measurements. Disagreement exists only for vibrational temperature (Fig. 4). As mentioned earlier, there is no evidence to support the theory that the measured vibrational temperature of an excited electronic state of N_2^+ should be the same as that of the ground state of N_2. Instead, there are several possible reasons why it could not be the same: The species N_2^+ itself is transient in nature and its concentration is out of equilibrium until all other reactions reach equilibrium (see Fig. 1), and hence, the quasi-steady-state conditions assumed in the NEQAIR program are never reached; the formation mechanism of the N_2^+ B state may be such that the vibrational levels are preferentially populated; and curve-crossing of the B state potential by several repulsive potentials may produce fast depletion of higher vibrational levels through predissociation, etc. To resolve this point, one of the following two steps must be taken: The vibrational temperature of the ground electronic state of N_2 could be measured experimentally, or a theory could be developed that independently calculates the vibrational temperature of the N_2^+ B state. If these data are excluded, the two-temperature kinetic model developed here is capable of reproducing the experimental data for velocities up to 6.4 km/s.

The relatively good agreement between the theory and experiment described in the present work is a significant improvement over previous studies.[4,8] This improvement can be attributed to the following: 1) Adoption of the latest vibrational relaxation model by Lee[21] according to which the relaxation rate is proportional to an sth power of the temperature difference $(T - T_v)$ [where s is determined by Eq. (1)]. 2) Use of the reaction rates based on the average temperature, Eq. (11). 3) For the lowest flow velocity considered, accounting for the electronic excitation of molecules by the collisions with heavy particles.

As described in the reaction model and indicated in Table 1, the reaction rate constants for the three reactions are more or less arbitrarily chosen. Of these three, the constants for the charge-exchange reaction are inconsequential: The rate is so fast that the process is most likely in local equilibrium, in which case the ratio of the number densities of the two ions involved becomes a function of temperatures and not a function of the rate coefficient. The same comment applies to the association ionization process. The multiplicative factor of 2 that was introduced for the electron-impact ionization process slightly improved the agreement between the theory and experiment. In view of the uncertainty existing in the rate coefficient value, modification of the rate coefficient by a factor of 2 may be considered tolerable. The largest uncertainty concerns the choice of the C value for the electron-impact dissociation reaction. In all plots of the relaxation, the final approach to equilibrium was seen to be dictated mostly by the choice of this value. The magnitude of the present C value is reasonable considering the fact that the vibrational excitation of N_2 by electron impacts occurs very rapidly.[21,22] Thus, the present choice of the rate coefficient values can be justified, provided the fundamental assumption of the present work is valid.

The fundamental assumption of the present work is that the dissociation rate coefficient values of Appleton et al.[19] that were used in the present work automatically account for the preferential high-vibrational-state depletion phenomenon (see the vibrational model section) in the present model. To be precise, the experimental data of Appleton et al. must be interpreted using the two-temperature model. Such reinterpretation is bound to increase the value of C. With this larger value of C, the exponent s in Eq. (2) will be different, and every aspect of the present findings will be affected. In particular, the theoretical vibrational temperatures will be lower than those shown in Fig. 4, thereby reducing the extent of discrepancy between the theoretical and the experimental data. Dissociation of N_2 has been studied experimentally in the past by using an interferometer that measured density changes accompanying dissociation.[30,31] This method gave higher rate coefficient values than those by Appleton et al. The rate coefficient values have also been deduced from the rates of production of the N atoms[32]; this computation gave even higher C values. It should be possible to deduce a consistent set of the constants corresponding to a two-temperature model from all these existing experimental data sets. Such work needs to be done in the future.

Conclusions

Using recent information and innovations, a two-temperature kinetic description of nitrogen has been formulated that enables one to numerically reproduce experimental data on radiative behavior behind normal shock waves in a shock tube up to a freestream velocity of 6.4 km/s. The theoretical vibration model, which accounts for the diffusive nature of vibrational relaxation but neglects preferential high-vibrational-state removal by dissociation, suggests that an

average temperature controls the dissociation rates and accounts for the electronic excitation of molecules during the collisions between a molecule and a heavy particle. The model approximately reproduces 1) translational-rotational temperature, 2) electronic excitation temperature, 3) temporal variation of radiation intensities, 4) characteristic relaxation times, and 5) the ratio of nonequilibrium- to equilibrium-radiative heat fluxes. The vibrational temperature of the ground electronic state of N_2 computed by this model does not agree with the measured vibrational temperatures of the B state of N_2^+. As there are no other vibrational temperature measurements available in the literature, direct verification of the present vibrational model could not be accomplished. Experimental measurement of vibrational temperature of the ground electronic state of N_2 is needed for ultimate validation of the present model.

References

[1]Walberg, G. D., "A Survey of Aeroassisted Orbit Transfer," *Journal of Spacecraft and Rockets*, Vol. 22, Jan.–Feb. 1985, pp. 3–18.

[2]Park, C., "A Review of Shock Waves Around Aeroassisted Orbital Transfer Vehicles," *Proceedings of the 15th International Symposium on Shock Waves and Tubes: Shock Waves and Shock Tubes*, D. Bershader and R. Hanson, eds., Stanford Univ. Press, Stanford, CA, 1986, pp. 27–41; also, NASA TM 86769, June 1985.

[3]Brahney, J. H., "Space Station's Biggest Challenge: Servicing Satellites in Orbit," *Aerospace Engineering*, Vol. 5, March 1985, pp. 9–13.

[4]Park, C., "Radiation Enhancement by Nonequilibrium in Earth's Atmosphere," *Journal of Spacecraft and Rockets*, Vol. 22. Jan.–Feb. 1985, pp. 27–36.

[5]Allen, R. A., Camm, J. C., and Keck, J. C., "Radiation from Hot Nitrogen," AVCO Everett Research Lab., Everett, MA, Research Rept. 102, April 1961.

[6]Allen, R. A., Keck, J. C., and Camm, J. C., "Nonequilibrium Radiation from Shock Heated Nitrogen and a Determination of the Recombination Rate," AVCO Everett Research Lab., Everett, MA, Research Rept. 110, June 1961.

[7]Allen, R. A., "Nonequilibrium Shock Front Rotational, Vibrational, and Electronic Temperature Measurements," AVCO Everett Research Lab., Everett, MA, Research Rept. 186, Aug. 1964.

[8]Park, C., "Problems of Rate Chemistry in the Flight Regimes of Aeroassisted Orbital Transfer Vehicles," in *Progress in Astronautics and Aeronautics, Vol. 96, Thermal Design of Aeroassisted Orbital Transfer Vehicles*, H. F. Nelson, ed., AIAA, NY, 1985, pp. 511–537.

[9]Park, C., "On Convergence of Computation of Chemically Reacting Flows," *Progress in Astronautics and Aeronautics, Vol. 103, Thermophysical Aspects of Re-Entry Flows*, J. N. Moss and C. D. Scott, eds., AIAA, Washington, DC, 1986, pp. 478–513.

[10]Park, C., "Calculation of Nonequilibrium Radiation in the Flight Regimes of Aeroassisted Orbital Transfer Vehicles," *Progress in Astronautics and Aeronautics, Vol. 96, Thermal Design of Aeroassisted Orbital Transfer Vehicles*, H. F. Nelson, ed., AIAA, Washington, DC, 1985, pp. 395–418.

[11]Park, C., "Nonequilibrium Air Radiation (NEQAIR) Program: User's Manual," NASA TM 86707, July 1985.

[12]Lee, J. H., "Basic Governing Equations for the Flight Regimes of Aeroassisted Orbital Transfer Vehicles," *Progress in Astronautics and Aeronautics, Vol. 96, Thermal Design of Aeroassisted Orbital Transfer Vehicles*, H. F. Nelson, ed., AIAA, Washington, DC, 1985, pp. 3–53.

[13]Appleton, J. P., "Shock-Tube Study of the Vibrational Relaxation of Nitrogen Using Vacuum-Ultraviolet Light Absorption," *Journal of Chemical Physics*, Vol. 47, Nov. 1967, pp. 3231–3240.

[14]Millikan, R. C. and White, D. R., "Systematics of Vibrational Relaxation" *Journal of Chemical Physics*, Vol. 39, Dec. 1963, pp. 3209–3213.

[15]Appleton, J. P., Steinberg, and Liquornik, D. J., "Shock-Tube Study of Nitrogen Dissociation Using Vacuum-Ultraviolet Light Absorption," *Journal of Chemical Physics*, Vol. 48, Jan. 1968, pp. 599–608.

[16]Baulch, D. L., Drysdale, D. D., and Horner, D. G., *Evaluated Kinetic Data for High Temperature Reactions. Vol. 2: Homogeneous Gas Phase Reactions of the H_2-H_2-O_2 System*, CRC Press, Cleveland, OH, 1973.

[17]Treanor, C. E. and Marrone, P. V., "The Effect of Dissociation on the Rate of Vibrational Relaxation," Cornell Aeronautical Lab., Buffalo, NY, Rept. QM-1626-A-4, Feb. 1972.

[18]Bray, K. N. C. and Pratt, N. H., "Conditions for Significant Gasdynamically Induced Vibration-Recombination Coupling," *Proceedings of 11th Symposium (International) on Combustion*, Combustion Institute, Pittsburgh, PA, 1967, pp. 23–36.

[19]Rich, J. W. and Rohm, R. G., "Population Distribution During Vibrational Relaxation of Diatomic Gas," *Proceedings of 11th Symposium (International) on Combustion*, Combustion Institute, Pittsburgh, PA, 1967, pp. 37–48.

[20]Keck, J. C. and Carrier, G., "Diffusion Theory of Nonequilibrium Dissociation and Recombination," *Journal of Chemical Physics*, Vol. 43, July 1965, pp. 2284–2298.

[21]Lee, J. H., "Electron-Impact Vibrational Excitation Rates in the Flow Field of Aeroassisted Orbital Transfer Vehicles," *Progress in Astronautics and Aeronautics, Vol. 103, Thermophysical Aspects of Re-Entry Flows*, J. N. Moss and C. D. Scott, eds., AIAA, Washington, DC, 1986, pp. 197–224.

[22]Huo, W. M., McKoy, V., Lima, M. A., and Gibson, T. L., "Electron-Nitrogen Molecule Collisions in High-Temperature Nonequilibrium Air," *Progress in Astronautics and Aeronautics, Vol. 103, Thermophysical Aspects of Re-Entry Flows*, J. N. Moss and C. D. Scott, eds., AIAA, Washington, DC, 1986, pp. 152–196.

[23]Jaffe, R. L., "Rate Constants for Chemical Reactions in High-Temperature Nonequilibrium Air," in *Progress in Astronautics and Aeronautics, Vol. 103, Thermophysical Aspects of Re-Entry Flows*, J. N. Moss and C. D. Scott, eds., AIAA, NY, 1986, pp. 123–151.

[24]Flagan, R. C. and Appleton, J. P., "Excitation Mechanisms of Nitrogen First-Positive and First-Negative Radiation at High Temperature," *Journal of Chemical Physics*, Vol. 56, Feb. 1972, pp. 1163–1173.

[25]Dunn, M. G. and Lordi, J. A., "Measurement of $N_2^+ + e$ Dissociative Recombination in Expanding Nitrogen Flows," *AIAA Journal*, Vol. 8, Feb. 1970, pp. 339–345.

[26]Park, C., "Measurement of Ionic Recombination Rate of Nitrogen," *AIAA Journal*, Vol. 6, Nov. 1968, pp. 2090–2094.

[27]Lotz, W., "Electron-Impact Ionization Cross-Sections and Ionization Rate Coefficients for Atoms and Ions from Hydrogen to Calcium," *Zeitschrift fur Physik*, Vol. 216, Oct. 1968, pp. 241–247.

[28]Allen, R. A., "Air Radiation Tables: Spectral Distribution Functions for Molecular Band Systems," AVCO Everett Research Lab., Everett, MA, Research Rept. 236, April 1966.

[29]Cooper, D. M., "Spectral Intensity Measurements from High-Pressure Nitrogen Plasmas," *Journal of Quantitative Spectroscopy and Radiative Transfer*, Vol. 12, July 1972, pp. 1175–1189.

[30]Cary, B., "Shock-Tube Study of the Thermal Dissociation of Nitrogen," *Physics of Fluids*, Vol. 8, Jan. 1965, pp. 26–35.

[31]Byron, S., "Shock-Tube Measurement of the Rate of Dissociation of Nitrogen," *Journal of Chemical Physics*, Vol. 44, Feb. 1966, pp. 1378–1388.

[32]Roth, P. and Thielen, K., "Measurements of N Atom Concentrations in Dissociation of N_2 by Shock Waves," *Proceedings of the 15th International Symposium on Shock Waves and Shock Tubes*, D. Bershader and R. Hanson, eds., Stanford Univ. Press, Stanford, CA, 1986, pp. 245–252.